Purification and Reconstitution of Sterol Transfer by Native Mouse ABCG5 and ABCG8[†]

Jin Wang,[‡] Da-wei Zhang,[‡] Ying Lei,[‡] Fang Xu,[§] Jonathan C. Cohen,[‡,§,||] Helen H. Hobbs,[‡,||,⊥,#] and Xiao-Song Xie*,[‡,||]

Eugene McDermott Center for Human Growth and Development, the Center of Human Nutrition, Departments of Internal Medicine and Molecular Genetics, and the Howard Hughes Medical Institute, University of Texas Southwestern Medical Center, Dallas, Texas, 75390-8591

ABSTRACT: ABCG5 (G5) and ABCG8 (G8) are ATP-binding cassette half-transporters that limit intestinal uptake and promote biliary secretion of neutral sterols. Here, we describe the purification of endogenous G5G8 from mouse liver to near homogeneity. We incorporated the native proteins into membrane vesicles and reconstituted sterol transfer. Native gel electrophoresis, density-gradient ultracentrifugation, and chemical cross-linking studies indicated that the functional native complex is a heterodimer. No higher order oligomeric forms were observed at any stage in the catalytic cycle. Sterol transfer activity by purified native G5G8 was stable, stereospecific, and selective. We also report that G5 but not G8 is S-palmitoylated and that palmitoylation is not essential for dimerization, trafficking, or biliary sterol secretion. Both G5 and G8 have short but highly conserved cytoplasmic tails. The functional roles of these C-terminal regions were examined using an *in vivo* functional assay.

ABCG5 (G5)[1] and ABCG8 (G8) are ABC half-transporters that limit the accumulation of neutral sterols in the body (*1*). The two proteins are expressed primarily in enterocytes and hepatocytes, where they heterodimerize in the endoplasmic reticulum prior to being transported to apical membranes (*1−3*). Inactivating mutations in either G5 or G8 cause sitosterolemia, a recessive disorder characterized by hyper-cholesterolemia, phytosterolemia, and premature coronary artery disease (*3, 4*). The role of G5 and G8 in sterol trafficking *in vivo* has been examined in detail using genetically modified mice, in which G5 and G8 are either overexpressed or inactivated (*5−10*). In the intestine, the G5G8 heterodimer limits the absorption of dietary sterols, especially plant-derived sterols (*5*). G5G8 synthesized in the liver is located in the bile canalicular membrane and is required for efficient secretion of neutral sterols into bile (*5*).

Previously, we developed an *in vitro* assay using recombinant G5G8 expressed in *Sf*9 cells to elucidate the mechanism by which G5G8 promotes translocation of sterols across membranes (*11*). Membrane vesicles prepared from *Sf*9 cells expressing wild-type G5 and G8 supported the transfer of cholesterol from donor vesicles. G5G8-mediated transfer was stereoselective and specific for neutral sterols. Introduction of mutations predicted to disrupt ATP hydrolysis abolished G5G8-mediated sterol transfer. The recombinant G5G8 transporter was purified to near homogeneity using affinity chromatography, and the purified heterodimer retained ATP-dependent sterol transfer activity when incorporated into proteoliposomes (*11*). These studies provided the first direct evidence that neutral sterols are the primary transport substrate for G5G8.

Recombinant G5G8 expressed in insect cells differs from the native complex in several respects, including post-translational modification, chaperone-assisted protein folding, and the addition of epitope tags used to facilitate purification. To characterize the native transporter, we have purified and functionally reconstituted G5G8 from mouse liver. To our knowledge, this is the first reconstitution of substrate transport by an ABC transporter purified from mammalian tissue.

EXPERIMENTAL PROCEDURES

Preparation of Postnuclear Membranes of Mouse Liver and Solubilization of G5G8. Mouse livers were weighed and washed with ice-cold buffer containing 50 mM Tris-HCl at pH 7.5, 50 mM NaCl, 0.5 mM ethylenediaminetetraacetic

* To whom correspondence should be addressed: The McDermott Center for Human Growth and Development MC8591, University of Texas Southwestern Medical Center, Dallas, TX 75390-8591. Telephone: 214-648-7700. Fax: 214-648-7720. E-mail: xiao-song.xie@utsouthwestern.edu.
‡ Eugene McDermott Center for Human Growth and Development.
§ Center of Human Nutrition.
|| Department of Internal Medicine.
⊥ Department Molecular Genetics.
Howard Hughes Medical Institute.

1 Abbreviations: ABC, ATP-binding cassette; G5, ABCG5; G8, ABCG8; Ab, antibody; BN, blue native; CMV, canalicular membrane vesicle; MCD, methyl-β-cyclodextrin; IP, immunoprecipitation; NBD, nucleotide-binding domain; OG, *n*-octyl β-D-glucopyranoside; PC, phosphatidylcholine; PE, phosphatidylethanolamine; PS, phosphatidylserine; PI, phosphatidylinositol; EGTA, ethylene glycol-bis(2-aminoethylether)-*N,N,N′,N′*-tetraacetic acid; MES, 2-(*N*-morpholino)ethanesulfonic acid; Tricine, *N*-[2-hydroxy-1,1-bis(hydroxymethyl)ethyl]-glycine; HEPES, *N*-2-hydroxyethylpiperazine-*N′*-2-ethanesulfonic acid; VO$_4$, vanadate.

acid (EDTA), and 1 mM dithiothreitol (DTT) (buffer A) prior to homogenization in a blender with 5 volumes of buffer A plus 1 μg/mL leupeptin, 1 μg/mL pepstatin and 0.5 mM phenylmethylsulphonyl fluoride (PMSF); all steps were performed at 4 °C. The homogenates were centrifuged at 1500g for 10 min, and the supernatants were further centrifuged at 100000g for 45 min. The resulting membrane pellets were stored at −80 °C.

To determine the best detergent for solubilization of G5G8, aliquots of mouse liver membranes (60 μg) were incubated with detergent (1%) for 1 h in a final volume of 30 μL. After centrifugation to remove insoluble materials, the supernatants were analyzed by sodium dodecyl sulfate−polyacrylamide gel electrophoresis (SDS−PAGE) and then subjected to immunoblotting. Successful solubilization was achieved using NP-40, Triton X-100, and $C_{12}E_9$ (data not shown). The nonionic detergent $C_{12}E_9$ was selected for use in these experiments because it does not absorb light at 280 nm.

To solubilize G5 and G8 for protein purification, membrane pellets prepared from 110 g (wet weight) of mouse liver were homogenized in 10 volumes of buffer A plus protease inhibitors (1 μg/mL leupeptin, 1 μg/mL pepstatin, and 0.5 mM PMSF) and 1% $C_{12}E_9$. The membrane suspension was incubated at room temperature for 15 min and then on ice for 45 min before centrifugation at 100000g for 1 h.

Isolation of Mature Native G5G8 from Mouse Liver. The mature, fully glycosylated form of G5G8 was separated from the immature form of the protein by sequential chromatography on Blue 4 and Blue 2 dye-affinity columns (Bio-Rad). Detergent extracts from the liver (1 L) were supplemented with 2 mM MgCl$_2$ and loaded onto a Blue 4 column (200 mL) equilibrated with 20 mM Tris-HCl at pH 7.5, 2 mM MgCl$_2$, 0.05% $C_{12}E_9$, 7.5% glycerol, and 1 μg/mL leupeptin (buffer E). The flow-through fraction was loaded onto a Blue 2 column (120 mL, equilibrated with buffer E) and washed extensively with 240 mL of the same buffer (minus MgCl$_2$). The mature form of G5 and G8 was eluted from the Blue 2 column with buffer E plus 2% Na−cholate and maintained at 4 °C. Most of the immature, ER form of G5 and G8 was recovered from the Blue 4 column by eluting with buffer E plus 1.5 M NaCl.

Purification of G5G8 by Ab-Affinity Chromatography. A polyclonal rabbit Ab raised against mouse G5 (*5*) was covalently linked to protein A-agarose beads (RepliGen) using an immobilization kit from Pierce. The Blue 2 column eluate was diluted 2× with buffer E (minus MgCl$_2$), mixed with 1 mL of the Ab−Protein A beads, and incubated at 4 °C overnight with slow rotation. The beads were packed into a column and washed extensively with 50 mL of buffer E plus 0.1 M NaCl. The bound proteins were eluted with 10 mL of ImmunoPure Gentle Ab/Ag elution buffer (Pierce) plus 0.05% $C_{12}E_9$. The initial 0.3 mL of the eluate was discarded, and the remainder was collected in 1 mL fractions and desalted using a desalting column (Bio-Rad) equilibrated with 20 mM Tris-Cl at pH 7.5, 50 mM NaCl, 0.05% $C_{12}E_9$, 7.5% glycerol, and 1 μg/mL leupeptin. The fractions were stored at −80 °C.

Reconstitution of Purified G5G8 into Proteoliposomes. The purified native G5G8 was reconstituted as previously described for the recombinant proteins synthesized in *Sf*9 cells (*11*) with modifications. In brief, 20 μL of the purified and desalted fractions, either obtained directly from the desalting

column or after being concentrated using a Microcon concentrator (Millipore), was mixed with 6 μL of Liposomes R stock solution prepared as described previously (*11*) (containing 600 μg of lipids) and 7 μL of reconstitution buffer (final concentration of 0.3 M sucrose, 0.15 M KCl, 2 mM MgCl$_2$, and 1 mM DTT). After vortexing, the mixture was incubated at room temperature for 1 h and then placed on ice. The proteoliposomes were used within 72 h of reconstitution.

Cholesterol-Transfer Assay. To determine if native G5G8 supported the transfer of cholesterol from donor liposomes to proteoliposomes containing the protein, we used a previously developed *in vitro* assay (*11*) with some modifications. Reconstituted purified G5G8 as described above (4−5 μL) was diluted at least 20-fold in 100 μL of buffer containing 20 mM Tris-Cl at pH 7.4, 2 mM MgCl$_2$, 100 mM NaCl, and 300 mM sucrose to seal the proteoliposomes. A total of 30 μL of donor liposomes (30 μg of lipids) containing ∼100 000 CPM/assay of [^{3}H]cholesterol, [^{3}H]cholesteryl oleate, or [^{3}H]phosphatidylcholine (PC) was added to the diluted proteoliposomes in 200 μL of assay solution containing 20 mM Tris-Cl at pH 7.4, 60 mM KCl, 30 mM NaCl, and 2 mM MgCl$_2$. The liposomes were incubated with the proteoliposomes at 37 °C for 60 min in the absence or presence of 5 mM ATP with or without the addition of an ATPase inhibitor, sodium vanadate (VO$_4$). At the end of the assay, the proteoliposomes containing G5G8 were separated from the donor liposomes by centrifugation as previously described (*11*). The ATP-dependent transfer of radiolabeled lipids from the donor liposomes to the proteoliposomes was measured by a scintillation counting of the precipitated proteoliposomes and was calculated by subtracting the counts transferred without ATP from those with ATP.

To examine the stereoisomeric specificity of substrate recognition, natural cholesterol and its hexadeuterated enantiomer were used as transport substrates in the assay. The transport assays were performed using PC liposomes as the donor, to which 1% of cholesterol or the hexadeuterated enantiomer of cholesterol (ent-cholesterol) was added. The assay was performed exactly as described for radioactively labeled cholesterol, except that the sterol transferred to the proteoliposomes was quantitated using gas chromatography−mass spectrometry (GC−MS). The amount of ATP-dependent sterol transfer was calculated as described for the experiments using radiolabeled lipids.

Loading of Methyl-β-cyclodextrin (MCD) into Proteoliposomes and Back-extraction of Cholesterol by CD. After reconstitution of purified G5G8 as described above, 15 mM MCD was added to the solution (20 mM Tris-HCl at pH 7.4, 2 mM MgCl$_2$, 100 mM NaCl, and 300 mM sucrose) with which the proteoliposomes were diluted and sealed.

To measure the accessibility of the MCD in the exterior solution to the transferred cholesterol after the reaction, transfer assays were performed exactly as described above, except that the centrifugation solution contained 15 mM MCD.

Adenovirus-Mediated Expression of G5 and G8 in Mice. Mice homozygous for disrupted alleles at *Abcg5* and *Abcg8* (G5G8$^{-/-}$) (*5*) were maintained on a regular chow diet (Harlan Teklad, Madison, WI). The knockout mice were infected with adenoviruses (5 × 10^{12} particles/kg injected into the tail vein) expressing either wild-type G5 and G8 or

mutant forms of the protein that were previously demonstrated to lack ATPase activity: G5 (K93M) and G8 (G216D) (*12*). After 72 h, the mice were fasted for 4 h, anesthetized with halothane, and killed by exsanguination. Liver tissue was removed and processed immediately as described below; bile samples were collected, and biliary neutral sterol levels were measured using GC−MS as described (*13*).

Preparation of Canalicular Membrane Vesicles (CMVs) from Mouse Liver. A total of 3 days after injection of the adenovirus, apical membrane vesicles were prepared from the livers by adapting a method used to isolate CMVs from rats (*14, 15*). The livers were removed (4 mice per group, total liver weight of 5−8 g) and perfused with a sucrose−*N*-2-hydroxyethylpiperazine-*N′*-2-ethanesulfonic acid (HEPES) buffer (SH buffer) containing 250 mM sucrose, 10 mM HEPES/Tris at pH 7.4, 1 mM PMSF, 2 μg/mL leupeptin, 2 μg/mL pepstatin, and 2 μg/mL aprotinin at 4 °C. The minced livers were homogenized on ice with a loose pestle 4 times in 25 mL of SH buffer supplemented with 0.2 mM $CaCl_2$ (SHCa buffer). The homogenate was filtered through 4 layers of gauze and then rehomogenized (15 strokes). The homogenate was suspended to 60 mL by addition of SH buffer plus EGTA (final concentration of 1 mM) and then subjected to centrifugation at 1880g for 10 min. The pellet was suspended in 20 mL of SHCa buffer and centrifuged at 3000g for 10 min. The resulting pellet was homogenized sequentially with a Polytron homogenizer in SHCa buffer for 30 s and then in a Waring blender for 3×15 s, followed by homogenization using a glass homogenizer for 6 strokes with a tight pestle. SHCa buffer was then added to the homogenate to a final volume of 60 mL and a final $CaCl_2$ concentration of 10 mM. After incubation on ice for 10 min, the suspension was centrifuged at 7600g for 20 min to remove any precipitate. The supernatant was further centrifuged at 47000g for 30 min, and the membrane pellet was collected. The homogenization−low speed spin−high speed spin cycle was repeated, and the final membrane pellet was suspended in SHCa buffer at a protein concentration of 3−5 mg/mL and stored at − 80 °C.

SDS−PAGE and Immunoblot Analysis. The membrane proteins were subjected to SDS−PAGE and Western blotting as described previously (*11*). The antibodies used for immunoblot analysis include rabbit polyclonal Abs against mouse G5 and G8, respectively (*5*), and a monoclonal anti-G8 Ab (1B10A5) raised against a recombinant peptide corresponding to amino acids 1−350 of G8 (*2*).

Blue Native (BN) Gel Electrophoresis and 2D Gel Electrophoresis. Blue native−polyacrylamide gel electrophoresis (BN−PAGE) was performed as described previously (*11*). Two-dimensional gel electrophoresis (2D gel) was performed using 0.75 mm BN−PAGE gels for the first dimension. The gel lanes were excised individually and placed horizontally on a SDS gel (1 mm). After the gel was run in the second dimension, immunoblotting was performed as described for one-dimensional gels (*11*). Protein concentrations were measured by either the DC protein assay kit (Bio-Rad) or protein staining in the gel.

Enzymatic Assays. ATP hydrolysis activity was measured in a 200 μL assay solution [50 mM Tris/2-(*N*-morpholino)-ethanesulfonic acid (MES) at pH 7.0, 30 mM KCl, 2.5 mM $MgCl_2$, and 2 mM [γ-^{32}P]-ATP (400 cpm/nmol)] in the absence or presence of VO_4. The ATP hydrolysis reaction

was performed at 37 °C for 1 h and terminated by addition of 1 mL of 1.25 N perchloric acid. Liberated $^{32}P_i$ was extracted and measured as detailed previously (*16*).

Alkaline phosphatase activity was determined by measuring the release rate of *p*-nitrophenol from *p*-nitrophenyl-5′-thymidylate as described (*17*).

Labeling Cells with [^{3}H]-Palmitic Acid. CRL-1601 cells were transfected with expression vectors containing G5 or G8 cDNA using the transfection reagent from Amaxa Biosystems according to the instructions of the manufacturer. After 48 h, the cells were metabolically labeled with [^{3}H]-palmitic acid (*18*). Briefly, the cells were washed once with PBS, preincubated for 2 h with 10 mL of Dulbecco's modified Eagle's medium (DMEM) containing 3.5% fatty-acid-free BSA (Roche) and 10 mM HEPES, and then labeled with 2 mCi [^{3}H]-palmitic acid for 4 h. Prior to use, [^{3}H]-palmitic acid (2 mCi, 5 mCi/mL) was dried under nitrogen and solubilized in 7 mL of serum-free DMEM containing 100 units/mL penicillin, 100 μg/mL streptomycin, and 3.5% fatty-acid-free BSA. The labeled cells were then washed once with ice-cold PBS and solubilized in 1 mL of lysis buffer (50 mM HEPES, 100 mM NaCl, 1.5 mM $MgCl_2$, 5 mM DTT, 1% (v/v) NP-40, 0.1% SDS, 5 mM EDTA, and 1× protease inhibitors). G5 and G8 were immunoprecipitated separately (*12*). Immunoprecipitated samples were fractionated by 8% SDS−PAGE followed by Western blotting or X-ray film exposure. For fluorography, gels were fixed in isopropanol/water/acetic acid (25:65:10) for 30 min, soaked in Amplify (Amersham Bioscience) for 1 h, dried under vacuum, and exposed to Kodak BioMax MS film (Kodak, Rochester NY) for 1 week at −80 °C.

For hydroxylamine treatment, the labeled cells were washed once with 20 mL of ice-cold PBS, broken by passing through a 25-gauge needle 20 times, and then treated with 1 M hydroxylamine (pH 7.0) or 1 M Tris-HCl (pH 7.0) for 2 h at 37 °C, followed by IP, SDS−PAGE, and autoradiography as described above.

Cell Culture. WIF-B cells were a generous gift from Ann Hubbard (Johns Hopkins University, Baltimore, MD) and were cultured as previously described (*19*).

Immunofluorescence Microscopy. The subcellular localization of ABCG5 and ABCG8 in cultured cells was determined by immunocytochemical analysis as described previously (*20*). Cells were imaged by confocal microscopy using a Zeiss LSM510 META 2P microscope.

Generation of Adenoviruses Expressing Truncated G5 and G8. Recombinant adenoviral vectors containing ABCG5-wt, ABCG5-T (deletion of amino acids 645−652), ABCG8-wt, ABCG8-T1 (deletion of amino acids 663−673), ABCG8-T2 (deletion of amino acids 666−673), and ABCG8-T3 (deletion of amino acids 669−673) were generated by *in vitro* cre-lox recombination. The adenovirus particles were used to express ABCG5 and ABCG8 in WIF-B cells that were cultured as described above. A total of 10 days following plating, cells were infected with 3.5×10^9 particles of virus per well in 12-well plates.

RESULTS

Functional Reconstitution of Cholesterol-Transfer Activity Using Mouse Liver Membrane Vesicles. Previously, we established a sterol transfer assay using inside-out membrane
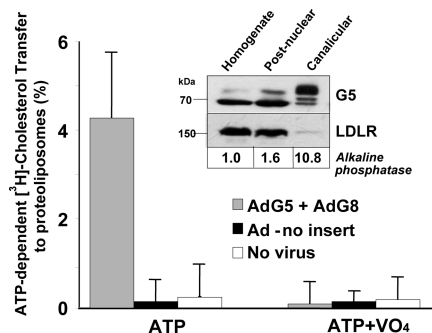
FIGURE 1: Reconstitution of cholesterol-transfer activity using mouse liver CMVs. CMVs were prepared from the livers of *G5G8*⁻/⁻ mice and from mice infected with adenoviruses that either express G5 and G8 or have no insert. Inside-out vesicles were made from the CMV- and ATP-dependent [³H]-cholesterol-transfer assays and were performed as described in the Experimental Procedures. (Inset) Immunblot analysis of G5 in the whole liver homogenate (25 μg), the postnuclear fraction (25 μg), and the CMVs (5 μg) of mice expressing G5 and G8 using a rabbit polyclonal antihuman G5 Ab (5). A total of 25 μg of protein from each fraction was subjected to immunoblotting using an anti-LDLR Ab (39). Alkaline phosphatase activity was measured as described in the Experimental Procedures using 25 μg of membrane protein.

vesicles containing recombinant G5G8 expressed in *Sf9* cells (21). When membrane vesicles isolated from mouse livers were used in the assay, only trace amounts of sterol transfer were observed (data not shown). Here, we isolated canalicular (apical) membranes from the livers of mice expressing high levels of recombinant G5 and G8 (6). Three G5G8 knockout mice were infected with adenoviruses expressing wild-type G5 plus wild-type G8 or an adenovirus containing no insert. Mice were sacrificed 3 days after the injection, and apical membrane vesicles were prepared from the livers using a protocol previously used to isolate CMVs from rat liver (15).

To assess the purity of the apical membranes, we examined the relative proportion of the ER form of the G5 in which the two N-linked sugars are not fully processed (apparent molecular mass of ∼70) to the mature, fully glycosylated form of the protein (molecular mass of ∼85 kDa) (1). Almost all of the immunodetectable G5 present in the apical membrane was the mature form of the protein (inset of Figure 1). The relative enrichment of the apical membrane fraction was assessed by measuring the activity of the apical membrane enzyme, alkaline phosphatase, which was substantially enriched. The low density lipoprotein receptor (LDLR) was markedly depleted in the canalicular membrane fraction, as expected for a basolateral membrane protein (inset of Figure 1).

The apical membrane vesicles obtained using this procedure were previously determined to be predominantly in a right-side-in orientation (15), so that the ATPases of G5 and G8 would be located in the lumen of the membrane vesicles. Therefore, the vesicles were disrupted using 1% octylglucoside (OG) and reconstituted, so that the NBDs of G5 and G8 were oriented to the outside of the vesicles (i.e., inside-out orientation) (11). ATP-dependent, VO₄-sensitive [³H]-cholesterol-transfer activity was observed in vesicles reconstituted from the CMVs of mice expressing recombinant G5 and G8 but not from those isolated from mice infected with the control virus (Figure 1). This finding demonstrated that G5G8-mediated cholesterol-transfer activity could be recon-
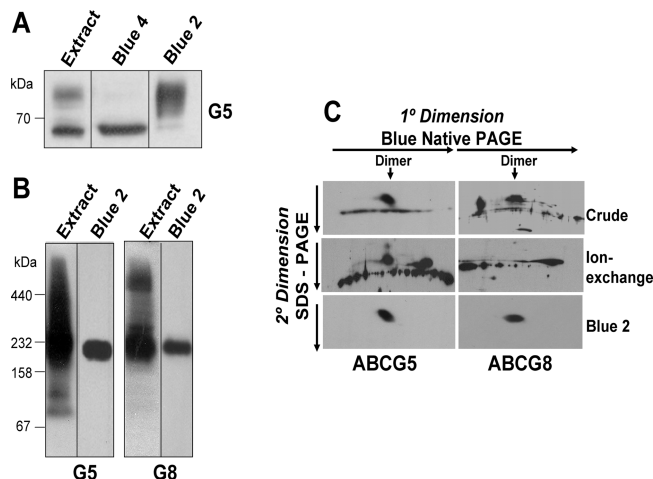

FIGURE 2: Solubilization of native G5G8 and separation of mature G5G8 from the immature forms of the half-transporters. Postnuclear liver membranes from wild-type mice were prepared and solubilized as described in the Experimental Procedures. (A) Immature (ER) and mature forms of G5 and G8 were separated by sequential Blue 4 and Blue 2 chromatography, as described in the Experimental Procedures. The crude detergent extract (25 μg), the proteins eluted from the Blue 4 column by 1.5 M NaCl and further purified by glycerol-gradient centrifugation (10 μg), and the Blue 2 column eluate (2 μg) were subjected with SDS−PAGE and immunoblotted with an anti-G5 Ab. (B) Oligomeric structure of G5 and G8 in the crude detergent extract and the Blue 2 column fraction from wild-type mouse livers. Crude detergent extract of wild-type mouse liver membranes (60 μg) and the Blue 2 column eluate (5 μg) were resolved by BN−PAGE and analyzed by immunoblotting using antibodies to G5 and G8. (C) Lanes from the gel shown in B containing the crude membrane extract and the eluate from the Blue 2 column were cut into strips and placed horizontally on a SDS−PAGE gel (10%). Also included in the experiment was an ion-exchange column (Mono Q) fraction of the crude extract. The SDS−PAGE was run as the second dimension and analyzed by Western blotting using anti-G5 and anti-G8 antibodies.

stituted from mouse livers. Further experiments were then performed to purify the native proteins.

Mature Native G5 and G8 Occur as a Heterodimer in Hepatic Canalicular Membranes. Both the mature and ER forms of native G5 and G8 were efficiently solubilized from the livers of wild-type mice using detergents with a similar polyoxyethylene structure: Triton X-100, NP-40, and $C_{12}E_9$. Chaps and OG were less effective at solubilizing the proteins (data not shown). For all subsequent experiments, $C_{12}E_9$ was used to solubilize native G5G8 from mouse liver.

Separation of mature G5G8 from the ER forms of the proteins was achieved by chromatography using a pair of blue dye-affinity columns (Figure 2A). The Blue 4 resin primarily adsorbed the ER form of G5 and allowed the mature, fully glycosylated form of the protein to pass through the column (Figure 2A). The Blue 2 column adsorbed both mature and ER forms of the proteins but with different elution profiles, such that sequential use of Blue 4 and Blue 2 columns effectively separated the two forms of the glycoprotein. Cholate (2%) but not salts or other detergents tested eluted G5G8 from the Blue 2 column without denaturing the complex (data not shown).

To determine the oligomeric structure of G5G8, the crude membrane extracts and the eluate from the Blue 2 column were subjected to BN gel electrophoresis and immunoblotting. A broad and heterogeneous distribution of immunoreactive bands was present in the crude membrane fraction
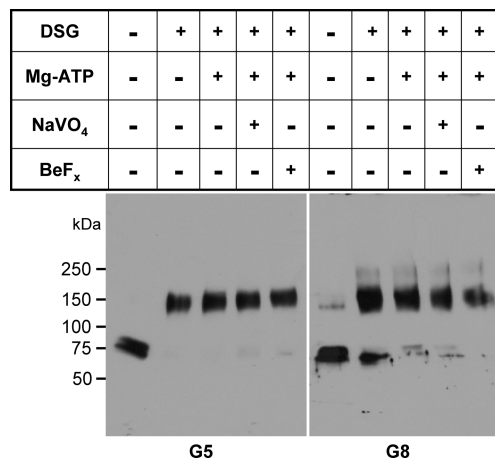
DSG	-	+	+	+	+	-	+	+	+	+
Mg-ATP	-	-	+	+	+	-	-	+	+	+
NaVO$_4$	-	-	-	+	-	-	-	-	+	-
BeF$_x$	-	-	-	-	+	-	-	-	-	+

FIGURE 3: Chemical cross-linking of the G5G8 complex. Partially purified native G5G8 (20 μg) that was obtained after fractionation over a Blue 2 column (see the Experimental Procedures) was incubated at room temperature for 15 min in the presence or absence of ATP (5 mM), MgCl$_2$ (2 mM), NaVO$_4$(1 mM), and BeF$_x$ (1 mM/5 mM). The proteins were then chemically cross-linked using disuccinimidyl glutarate (DSG) according to the instructions of the manufacturer. The proteins were then analyzed by SDS−PAGE and Western blotting.

(Figure 2B), with a major broadband of ∼200 kDa that probably represents the G5G8 dimer. The heterogeneous pattern of bands presumably reflects the presence of both the immature and the fully glycosylated proteins in monomeric form as well as in complexes with the ER chaperone protein calnexin (*22*). In striking contrast to these results, after sequential Blue 4 and Blue 2 chromatography, the proteins were recovered almost exclusively as dimers. The native G5 and G8 complex in the Blue 2 fraction was functionally active as indicated by its ability to catalyze ADP-trapping and cholesterol transfer (data not shown).

When the BN−PAGE resolved gel strip was further analyzed by SDS−PAGE, the mature forms of both G5 and G8 were seen exclusively at the dimer position (Figure 2C), whereas the ER form of G5 showed a heterogeneous pattern that spanned a wide molecular-weight range, likely because of the association with ER chaperone proteins (*22*).

The solubilized crude membrane fraction from the Blue 2 column was subjected to density-gradient centrifugation. The immature forms of the glycoproteins were present in multiple fractions, whereas the mature forms of G5 and G8 were present predominantly in the same two fractions (data not shown). The apparent molecular mass of the mature forms of the protein was ∼158 kDa, which corresponds to the expected size of a heterodimer.

To determine if the oligomeric structure of G5G8 changes during the catalytic cycle, we performed cross-linking experiments in the presence or absence of Mg−ATP and inhibitors, including NaVO$_4$ and BeF$_x$. The cross-linked G5G8 migrated as a dimer on SDS−PAGE. No higher molecular-weight forms of the proteins were observed under the conditions examined (Figure 3).

Although the mature form of G5G8 was separated from the ER form by Blue dye-affinity chromatography, it was only partially purified, even after the fractions were subjected to size fractionation using glycerol-density-gradient centrifugation or gel-filtration chromatography (data not shown). Other purification techniques, such as chromatography with
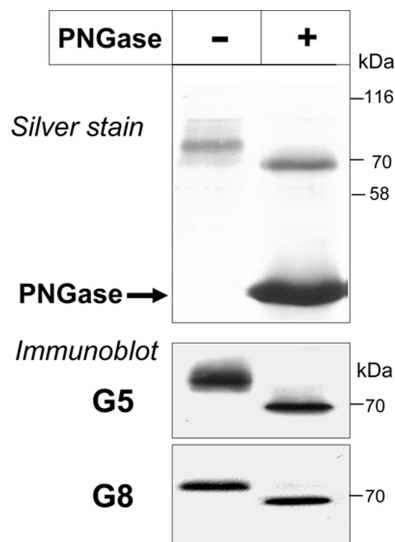

FIGURE 4: Purification of native mouse G5G8 by G5 Ab-affinity chromatography. Native G5G8 was affinity-purified using G5 Ab-conjugated beads as described in the Experimental Procedures. An aliquot of the purified protein (25 ng) was treated with peptide N-glycosidase F (PNGase), and the proteins were size-fractionated on a 12.5% SDS−PAGE before the gel was stained with silver (top) or analyzed by Western blotting (0.5 ng of protein) using anti-G5 and anti-G8 antibodies (bottom).

ion exchange or hydroxyapatite columns, were also tested but were found to disrupt the dimer [see the fraction from ion-exchange (Mono Q) chromatography in Figure 2C].

Purification of G5G8 by Ab-Affinity Chromatography. Native G5G8 was purified to near homogeneity using affinity chromatography with G5 Ab-conjugated beads (top of Figure 4). Treatment of the purified proteins with peptide N-glycosidase F (PNGase) decreased the apparent molecular mass by the expected amount and did not generate additional bands. No other proteins were identified that copurified with G5G8 in a stoichiometric manner. The identity of the proteins was confirmed by immunoblotting with anti-G5 and anti-G8 antibodies (bottom of Figure 4).

Functional Reconstitution of Purified Native G5G8. Purified native G5G8 was reconstituted into proteoliposomes and assayed for sterol-transfer activity. Positive and negative controls for the assay were established using adenovirally expressed recombinant wild-type or mutant G5G8 purified from the livers of *G5G8*$^{-/-}$ mice (Figure 5A). Solubilization and purification of the recombinant proteins was performed using exactly the same Ab-affinity chromatography procedure used for endogenous G5G8. Under the experimental conditions used, the sterol-transfer activity of native G5G8 and recombinant wild-type G5G8 was essentially identical (Figure 5B). ATP-dependent cholesterol transfer by the native G5G8 complex required Mg^{2+} and was inhibited by vanadate (data not shown). The ATP-dependent, VO$_4$-sensitive cholesterol-transfer activity was directly related to the amount of native G5G8 in the assay (Figure 6A) and was linear for the first 90 min of the assay (Figure 6B).

From these data, we estimated the transfer rate of cholesterol to be 0.6 μmol mg^{-1} min^{-1}, although this may be an overestimate if the radioactive cholesterol probe is preferentially transferred.

Sterol-Transfer Activity of G5G8 Is Stereoselective. Previously, G5G8 expressed in insect cells mediated transfer of
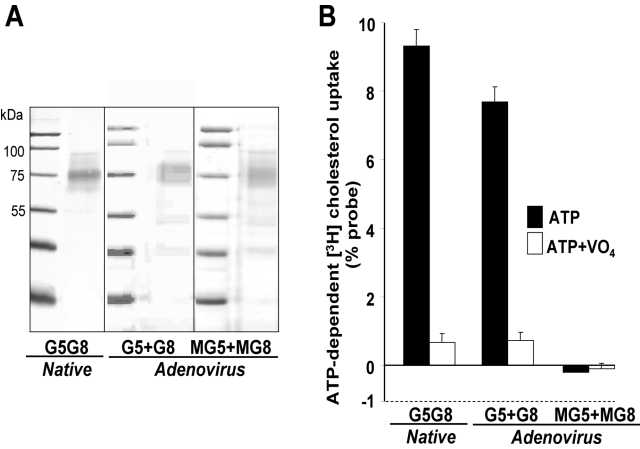
FIGURE 5: Reconstitution of purified G5G8 into proteoliposomes and measurement of ATP-dependent cholesterol transfer. (A) Native and recombinant G5 and G8 (both wild-type and mutant) were purified from the livers of *G5G8*^{-/-} mice by affinity chromatography as described in the Experimental Procedures. A total of 20 ng of protein was resolved on a 12.5% SDS−PAGE gel, and the gel was stained with silver as described in the Experimental Procedures. (B) ATP-dependent [³H]-cholesterol transfer was performed as described in the Experimental Procedures using proteoliposomes (15 ng) containing G5G8 purified from wild-type mice (native G5G8) or *G5G8*^{-/-} mice infected with adenoviruses expressing wild-type G5 and G8 or mutant forms of G5 and G8 (MG5 and MG8) that fail to hydrolyze ATP. The ATP-dependent [³H]-cholesterol-transfer activity was calculated from the difference between the signals measured in the presence of ATP ± addition of the inhibitor vanadate (VO₄).
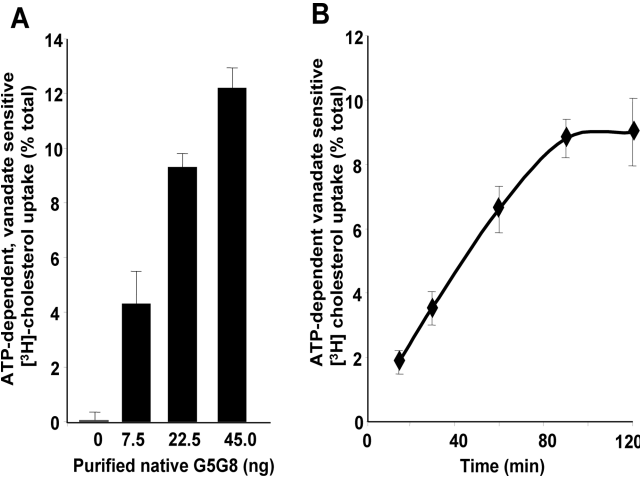

FIGURE 6: Protein concentration dependence and time course of cholesterol-transfer activity by purified native mouse G5G8. (A) Purified native G5G8 prepared as described in the Experimental Procedures was concentrated using a Microcon filter (Amicon) and reconstituted into proteoliposomes. In this assay, the concentration of G5G8 was such that the same volume of proteoliposomes was used for each cholesterol uptake assay. ATP-dependent cholesterol transfer was measured as described in Figure 5. (B) Time course of ATP-dependent cholesterol uptake was determined by measuring ATP-dependent [³H]-cholesterol transfer from the donor liposomes to the proteoliposomes containing native G5G8 (20 ng) at the designated time intervals.

the enantiomer of cholesterol (ent-cholesterol) as well as cholesteryl oleate and phosphotidylcholine (PC) at low but clearly detectable levels (*11*). Transfer of these substrates was not sensitive to VO₄. In contrast, native G5G8 did not mediate any detectable ATP-dependent transfer of these compounds (data not shown).

Table 1: Effect of Phospholipids and Sterols on ATPase Activity of Native G5G8 Isolated from Mouse Liver[a]

lipid (2.5 μg)	G5G8 ATP hydrolysis activity [μmol (mg of protein)⁻¹ min⁻¹]
none	0.39 ± 0.05
phosphotidylcholine	0.38 ± 0.01
phosphotidylserine	0.35 ± 0.10
cholesterol	0.20 ± 0.02
sitosterol	0.21 ± 0.05
lipid mixture, as described in the Experimental Procedures	0.33 ± 0.10

[a] Sterols in ethanol (100%) were added to a glass tube and dried under N₂. Purified native G5G8 (35 ng) and the assay buffer were added to the tube, and the sterols were suspended by gentle mixing using a pipet. The individual phospholipids and cholesterol/phospholipid mixtures were prepared as liposome solutions and added directly to the assay mixture. For each assay, the ATP hydrolysis activity of purified G5G8 was measured after incubation at 37 °C for 60 min in the presence or absence of the lipid, as described in the Experimental Procedures. A parallel set of tubes containing only the lipid served as controls for the experiments. The background counts from the lipid-alone controls were subtracted from the values obtained after addition of the enzyme to obtain the G5G8-dependent ATPase activity.

A crucial question that we have attempted to address using multiple different approaches is whether G5G8 catalyzes not just the transfer but also the trans-bilayer transport of sterols from the liposomes to the vesicle. We performed experiments in which we incorporated MCD into the interior of proteoliposomes to function as a cholesterol acceptor. We then incubated the proteoliposomes with sterols and assayed for the ability to back extract the sterols into the medium. A small fraction of the cholesterol transferred to the liposomes by G5G8 was not back-extracted by MCD under the assay conditions tested, but this fraction was not increased by incorporating MCD into the lumen of the liposomes (data not shown). Thus, we were unable to demonstrate G5G8-mediated transport of sterol across a lipid bilayer using this assay system.

ATPase Activity of Purified Native G5G8 Is Not Stimulated by Sterols. The ATPase activity of purified native G5G8 was 0.39 μmol of ATP mg⁻¹ min⁻¹ (Table 1), which was approximately 3-fold higher than that seen using recombinant proteins expressed in insect cells (*11*). The ATPase activity was not stimulated by the addition of cholesterol, sitosterol, or phospholipids, either individually or in combination. Unlike ABCG2 and most other ABC transporters (*23*), the ATPase activity was mildly but consistently *inhibited* rather than stimulated by its substrates (e.g., cholesterol and sitosterol). Interestingly, Takahashi et al. (*24*) reported that the ATPase activity of another sterol transporter, ABCA1, is slightly inhibited by the addition of cholesterol.

Palmitoylation of G5. We have previously reported that G5 and G8 are glycosylated and that glycosylation of G8 is essential for cellular trafficking (*22*). To determine if other types of protein modifications are required for G5G8 function, we tested for fatty acylation modification of the transporter. We used transient transfection to express the two half-transporters in cultured rat hepatoma cells (CRL-1601) labeled with [³H]-palmitic acid. The cells were lysed, and G5 and G8 were immunoprecipitated from a solubilized membrane fraction. As shown in Figure 7A, a band corresponding to the mature form of G5 was labeled with [³H]-palmitic acid in cells expressing both G5 and G8. No labeling
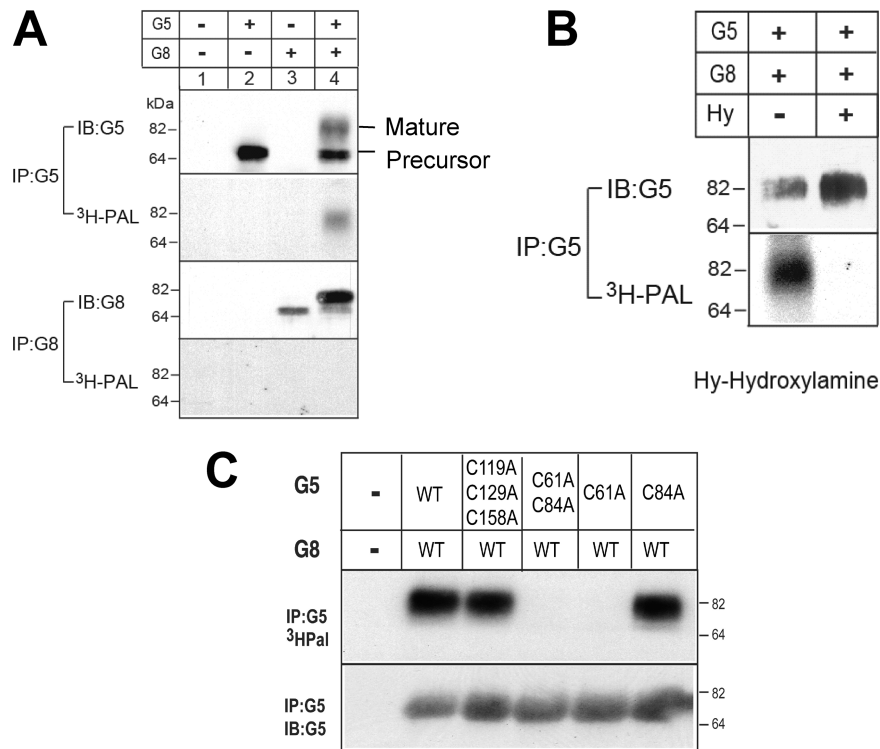
FIGURE 7: Palmitoylation of G5. (A) Recombinant G5 and G8 were transiently expressed in CRL-1601 hepatocytes. A total of 48 h after transfection of the expression plasmids, the cells were metabolically labeled with [³H]-palmitic acid. The cells were solubilized in 1 mL of lysis buffer, and G5 and G8 were immunoprecipitated using anti-G5 and anti-G8 specific antibodies. Immunoprecipitated samples were separated by 8% SDS−PAGE followed by immunoblotting or X-ray film exposure (7 days). (B) Labeled cells were washed once with 20 mL of ice-cold PBS, broken by passing through a 25-gauge needle 20 times, and then treated with 1 M hydroxylamine (pH 7.0) or 1 M Tris-HCl (pH 7.0) for 2 h at 37 °C, followed by IP, SDS−PAGE, and Western blotting or X-ray film exposure. (C) Site-directed mutagenesis was used to substitute selected cysteines predicted to be located in the cytoplasmic regions of G5 with alanine. The effect of these substitutions on palmitoylation was assayed as described above.

of G8 was seen in these cells or in cells infected with either G5 alone or G8 alone.

To confirm that palmitate was covalently linked to G5, duplicate [³H]-palmitate-labeled samples were subjected to treatment with either 1 M hydroxylamine, which cleaves thioesterified fatty acids (*25*), or Tris-HCl buffer. As shown in Figure 7B, [³H]-palmitate labeling of G5 was eliminated by treatment with hydroxylamine and not by Tris-HCl buffer, indicating that the labeling was due to palmitoylation at a cysteine residue(s) via a thioester bond. We then used site-directed mutagenesis to identify a single cysteine, Cys 61, in the N-terminal cytoplasmic region of G5 as the residue that is acylated (Figure 7C).

The role of G5 palmitoylation in G5G8 intracellular transport and biliary secretion of cholesterol and plant sterol was examined using an *in vivo*, adenovirus-based expression system as described previously (*12*). Substitution of alanine for cysteine 61 in G5 (C61A) did not adversely affect trafficking of G5G8 (Figure 8A) or biliary excretion of cholesterol or plant sterol levels (Figure 8B).

Role of the Cytoplasmic Tails of G5 and G8. Both G5 and G8 have short C-terminal tails (9 and 11 residues, respectively) that are highly conserved across species (Figure 9A). We used mutagenesis to delete the four terminal residues from the C-terminal tail of G5 (G5-T), and we made a series of truncations in G8 (G8-T1, G8-T2, and G8-T3) (Figure 9B). First, we examined whether the terminal sequences of G5 and G8 are required for translocation of the complex to the apical membrane.
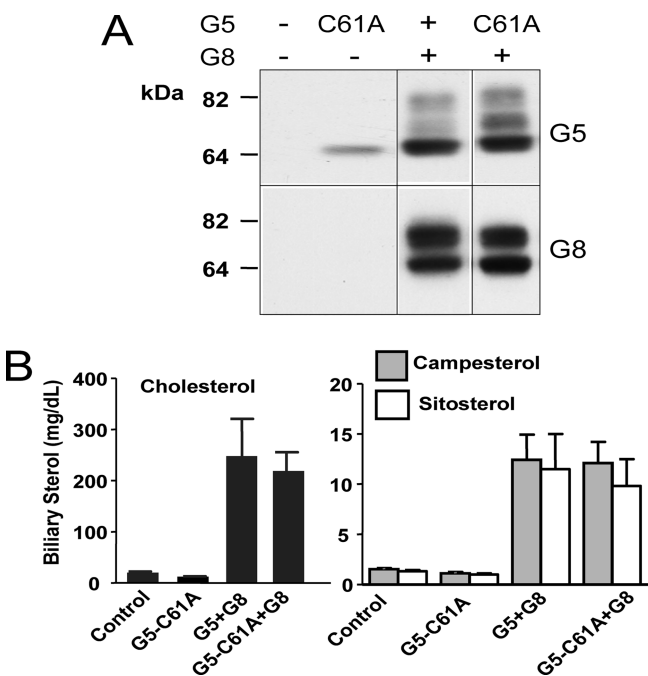

FIGURE 8: Functional analysis of the palmitoylation of G5. *G5G8⁻/⁻* mice were infected with adenoviruses encoding wild-type or mutant G5 (C61A) and wild-type G8 (8 mice/group). (A) Immunoblot analysis of liver membrane fractions from a representative mouse from each group was performed using antibodies to mouse G5 (4591) and G8 (1B10A5). (B) Gallbladder bile was collected following a 4 h fast, and biliary cholesterol was measured using GC−MS, as described in the Experimental Procedures.
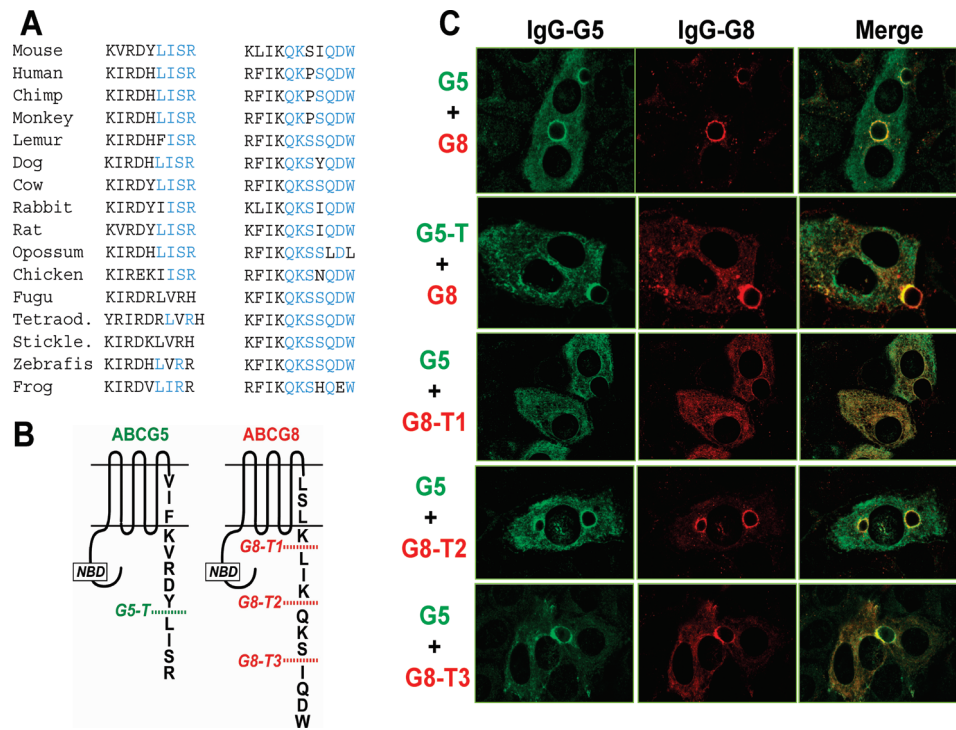
FIGURE 9: Effects of C-terminal truncations of G5 and G8 on subcellular localization in polarized hepatoctyes. (A) Sequence comparison of the C-terminal tails of G5 and G8 from 16 different species. Regions that were deleted in these studies and had no consistent qualitative effect on protein localization are highlighted in blue. (B) Site-directed mutagenesis was used to introduce premature stop codons into the C-terminal domains of G5 and G8 at the locations indicated. (C) WIF-B cells were grown on glass coverslips, infected with the indicated recombinant adenoviruses, and processed for immunofluorescence microscopy. Fixed and permeabilized WIF-B cells were incubated with anti-G5 pAb (4591) and anti-G8 mAb (1B10A5), followed by goat anti-rabbit Alexa 488 and anti-mouse Alexa 568, respectively. Cells expressing G5 and G8, G5-T and G8, G5 plus either G8-T1, G8-T2, or G8-T3 are shown. Colocalization is shown as a merged image.

As we have previously reported, co-expression of G5 and G8 in WIF-B cells, a polarized cultured hepatocyte cell line (*19*), results in transport of the proteins to the apical membrane (*1*)(Figure 9C). Co-localization of the proteins in apical membranes was also observed in WIF-B cells expressing G5-T and G8. Thus, the terminal four amino acids of G5 are not required for trafficking of the proteins to the apical membrane. Next, we co-expressed wild-type G5 with G8-T1, G8-T2, or G8-T3. G8-T2 and G8-T3 supported apical localization when co-expressed with wild-type G5, whereas G8-T1 failed to be transported to the apical membrane when expressed with wild-type G5 (Figure 9C).

To examine the effects of the C-terminal deletion on sterol transport, we used recombinant adenoviruses to express each construct in $G5G8^{-/-}$ mice. The results of immunoblot analysis of G5 and G8 in the livers of these mice were consistent with the localization studies in WIF-B cells. No mature G5 or G8 was detected in the livers of mice expressing wild-type G5 and G8-T1 (Figure 10A). In contrast to these results, the mature forms of both proteins were present in the livers of the other animals, albeit in varying relative amounts (because G5 expression tended to be higher than G8 expression, the relative amount of immature to mature G5 tended to be greater).

The amount of biliary cholesterol tended to correlate with the relative amount of mature G5 and G8 seen by immunoblotting (Figure 10B). Biliary cholesterol levels in mice expressing wild-type G5 and G8-T1 were comparable to those of knockout animals, whereas expression of the other three mutations was associated with significantly higher biliary sterol levels. These data indicate that the terminal 4
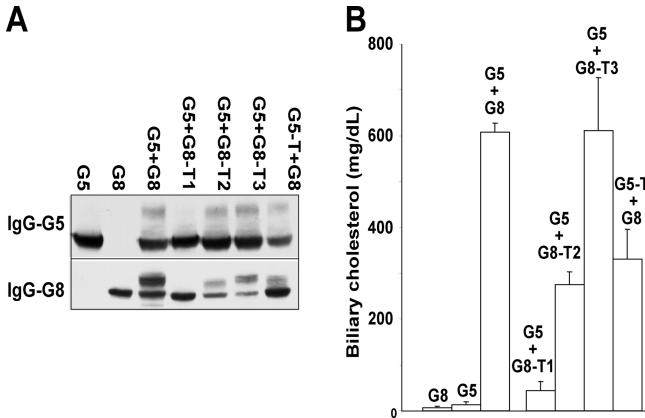

FIGURE 10: Effects of C-terminal deletion of G5 or G8 on biliary sterol secretion *in vivo*. $G5G8^{-/-}$ mice were infected with adenoviruses encoding wild-type or truncated G5 and G8 (3 mice/group). (A) A total of 3 days after infection, liver samples from these mice were pooled and subjected to immunoblotting as described in the Experimental Procedures. (B) Gallbladder bile was collected from these mice following a 4 h fast, and biliary cholesterol was measured using GC−MS. This experiment was repeated once, and similar results were obtained.

amino acids of G5 and the terminal 7 amino acids of G8 are not essential for targeting the transporter to the apical membrane or the secretion of sterols into bile (Figure 9A). Our data do not exclude the possibility that these terminal sequences contribute to the efficiency of either the trafficking or the sterol transport activity of G5 and G8, which may not be detected by the *in vivo* assay system used in these experiments.

DISCUSSION

In this paper, we describe the first purification and functional reconstitution of native G5G8. The native proteins were co-purified as a heterodimer, and we found no evidence for higher order oligomerization. Previously, we showed that recombinant, epitope-tagged forms of G5G8 expressed in insect cells promote the transfer of sterols from donor vesicles to proteoliposomes. Here, we demonstrated that sterols are the direct transport substrates of native G5G8. Native G5G8 was significantly more stable than the recombinant transporter, which allowed for more detailed biochemical characterization of the transporter.

The stoichiometric amount of ATP hydrolyzed by ABC transporters per allocrite translocation event is a major unresolved question. Models proposing hydrolysis of one or two ATP molecules per transport cycle have been put forward (26), but measured ratios of ATPase activity to allocrite transport vary widely, even for the same transporter (27–30). In our previous study using purified recombinant G5G8, sterol-transfer activity was not sufficiently stable over time to allow for a quantitative estimate of the allocrite transfer rate. In the present study, the native purified complex maintained linear cholesterol-transfer activity of 0.1% of labeled cholesterol per minute for over 90 min (Figure 6B). Assuming that the labeled cholesterol traces all of the cholesterol in the donor particle, this activity represents a transfer rate of 0.6 μmol of cholesterol (mg of G5G8)$^{-1}$ min^{-1}. The ATPase activity of the native complex was 0.39 μmol mg^{-1} min^{-1}, suggesting a coupling ratio of 1 ATP molecule hydrolyzed per sterol molecule translocated. This ratio cannot be considered definitive, because both the sterol transfer rate and the ATPase activity of the reconstituted transporter are subject to measuring errors. Nonetheless, a coupling ratio of 1:1 is consistent with our earlier observation that only one of the nucleotide-binding domains of the G5G8 complex hydrolyzes ATP (12).

Our current knowledge concerning the mechanisms of action of ABC transporters has been inferred almost entirely from recombinant proteins expressed in heterologous cells or membranes. Few studies have examined in detail the function of native ABC transporters. An exception is ABCR (ABCA4), which was purified from bovine rod outer segments (27). Although the putative substrate, all-*trans* retinal, increased ATPase activity of the transporter, Sun et al. did not report retinal transport by the purified protein (27). Mao et al. (28) purified native MRP1 (ABCC1) from doxorubicin-selected cultured lung tumor cells and reconstituted active transport of cysteinyl leukotriene C, an endogenous substrate of the transporter. Thus, the present study describes the first purification and reconstitution of substrate transport by a mammalian ABC transporter purified from the tissues in which it is expressed.

Although the use of recombinant proteins has many experimental advantages, the fidelity with which they reflect the properties of the native protein is uncertain. Differences in post-translational modifications, protein folding, and complex assembly may affect the properties of the recombinant protein. Although the results that we obtained using the native protein purified from mouse liver were qualitatively similar to those obtained using the recombinant protein produced in *Sf9* cells, use of the native complex had several advantages. A major advantage of using the native protein was its stability. Previously, we have used membrane vesicles from recombinant *Sf9* cells for our functional studies because the purified recombinant proteins produced in these cells is highly unstable. The purified insect-G5G8 is freeze-labile and loses activity within 24 h, even after it is reconstituted into proteoliposomes. In contrast, reconstituted native G5G8 retains maximal activity for several days when maintained at 4 °C (data not shown). The G5G8 purified from the liver can be stored at −80 °C and undergoes freeze−thawing up to 3 times without any reduction in sterol-transfer activity (data not shown). In addition, the purified complex can be concentrated 10-fold using Microcon filters (Millipore) without inducing aggregation.

Another difference between the insect-derived and native G5G8 was in the selectivity of lipid transport. Recombinant G5G8 synthesized in insect cells consistently transferred small amounts of cholesteryl esters and phospholipids, whereas essentially no ATP-dependent transfer of these molecules was observed when the native protein was used in the same assays. The results of these experiments demonstrate the strict substrate selectivity of G5G8. Furthermore, the present results confirm that G5G8-mediated transfer of cholesterol is exquisitely stereoselective; we observed no ATP-dependent transfer of the enantiomer of cholesterol by native G5G8. We do not know if the observed differences between the recombinant and native proteins are attributable to differences in glycosylation of the proteins expressed in insect versus mammalian cells, the presence of epitope tags at the C termini of the recombinant proteins, or to other yet-to-be-identified factors.

Recombinant G5 and G8 were co-purified as a heterodimer from *Sf9* cells, consistent with current structural models of ABC transporters (29). Higher order oligomeric structures have recently been reported for ABCG2 (30) and ABCA1 (31). Interestingly, ABCA1 appeared to transition from a dimer to a higher order oligomer during the catalytic cycle (31). We used native gel electrophoresis, density-gradient ultracentrifugation, and chemical cross-linking studies to examine the oligomeric structure of native G5G8. All three methods indicated that the functional complex is a heterodimer, and no higher order oligomeric forms were observed at any stage in the catalytic cycle.

ATPase activity is stimulated by the addition of the transport substrate for most ABC transporters (36, 37). In our previous study using recombinant G5G8 expressed in insect cells, cholesterol appeared to cause a slight reduction in ATPase activity but the functional instability and low activity of the purified recombinant protein made it difficult to obtain consistent ATPase measurements (11). The stable activity of purified native G5G8 provided us with an opportunity to address this issue more definitively. Here, we have confirmed a mild but consistent inhibition of G5G8 ATPase activity by both cholesterol and sitosterol. A similar phenomenon was reported for ABCA1; the ATPase activity of this cholesterol transporter is also slightly inhibited by the addition of sterol (24). It is possible that the addition of cholesterol to the membrane in the absence of an acceptor affects ATPase activity by altering the conformation of the protein. *In vivo*, mixed micelles of PC/bile acids serve as the natural acceptor for cholesterol transport to the bile. Further studies will be required to determine the effect of

cholesterol-binding on the conformation of the NBDs in the G5G8 transporter.

We also demonstrated that G5 but not G8 is palmitoylated through a thioester linkage at C61 (Figure 7). Only the mature form of G5 is palmitoylated, indicating that the modification occurs after the protein leaves the ER, presumably in the Golgi. Studies in yeast have shown that protein palmitoylation is catalyzed by a family of cysteine-rich Asp-His-His-Cys (DHHC) domain-containing proteins (DHHC proteins) (*32*). Of 23 predicted DHHC proteins in the human genome (*33*), Fernández-Hernando et al. reported that DHHC-2, -3, -7, -8, and -21 were co-localized with the Golgi matrix protein GM-130 in COS-7 cells (*34*). Therefore, it is possible that some of these DHHC proteins are involved in the palmitoylation of G5.

This is the first ABC transporter demonstrated to be palmityolated. In other proteins, palmitoylation has been shown to modulate protein−protein interactions and enzymatic activity as well as promote subcellular trafficking and interaction with the cell membrane (*35*). Although the functional role of palmitoylation of G5 is not clear, we have shown that the modification is not required for heterodimerization, trafficking of the protein to the apical membrane, or function of the complex.

The architecture of ABC transporters includes two NBDs that catalyze the hydrolysis of ATP and two transmembrane domains that are believed to mediate substrate binding and transport. Much less is known about the role of the short C-terminal, cytoplasmic regions of the proteins. The cytoplasmic tails of some ABC transporters may be important for their subcellular localization. For example, the C-terminal regions of CFTR and MRP2 contain PDZ-interacting motifs that may play a role in sorting to the apical membrane. It has also been demonstrated that the removal of only two or three amino acids from the C terminus of ABCG2 was enough to cause impaired trafficking of the transporter (*36*).

G5 and G8 are transported efficiently and specifically to the apical membrane of both hepatoctyes and enterocytes, yet the signals that target the heterodimer to the apical membrane are not known. In the current study, we examined whether the C-terminal regions of G5 and G8 contribute to localization of the transporter. Both of the C-terminal cytoplasmic regions of G5 and G8 are highly conserved across species (Figure 9A), although neither half-transporter contains a consensus sequence for established membrane targeting motifs, such as a PDZ-binding domain or a tyrosine motif. Surprisingly, despite strong conservation of the terminal 4 amino acids of G5 and the 7 amino acids of G8, these sequences were not essential for heterodimerization, apical trafficking, or sterol-mediated transport of G5G8. We cannot rule out that these sequences have more subtle effects on protein trafficking or function that were not detected using our methods.

We have shown that G5G8 can promote the transfer of cholesterol between membranes, but it is not known if the complex directly mediates movement of cholesterol from an intracellular donor to the apical membrane, from the inner to the outer leaflet, or across the bilayer to an acceptor (*37, 38*). To determine if G5G8 can directly mediate cholesterol transport across the membrane bilayer, we attempted to trap cholesterol in the interior of proteoliposomes using methyl-β-cyclodextrin (MCD). We were unable to demonstrate MCD-dependent sequestration of cholesterol in this assay. It is possible that the MCD-binding sites were already saturated with cholesterol before the assays were performed. Cholesterol from liposomes trapped with MCD during the formation of the proteoliposomes or cholesterol extracted from the membrane lipids, which have a high liposomes/protein ratio, could saturate the MCD-binding sites.

Our failure to demonstrate G5G8-mediated trans-bilayer transport may reflect inadequacies in our assay conditions. Alternatively, it may indicate that the true function of G5G8 is to transfer cholesterol to the membrane or between leaflets of the membrane rather than to transport cholesterol across the membrane. Further studies will be required to elucidate the molecular mechanism by which G5G8 promotes cholesterol secretion. The purification of a stable, functional G5G8 complex provides a valuable reagent with which to pursue these studies.

REFERENCES

1. Graf, G. A., Li, W.-P., Gerard, R. D., Gelissen, I., White, A., Cohen, J. C., and Hobbs, H. H. (2002) Coexpression of ATP-binding cassette proteins ABCG5 and ABCG8 permits their transport to the apical surface. *J. Clin. Invest. 110*, 659–669.
2. Graf, G. A., Yu, L., Li, W. P., Gerard, R., Tuma, P. L., Cohen, J. C., and Hobbs, H. H. (2003) ABCG5 and ABCG8 are obligate heterodimers for protein trafficking and biliary cholesterol excretion. *J. Biol. Chem. 278*, 48275–48282.
3. Berge, K. E., Tian, H., Graf, G. A., Yu, L., Grishin, N. V., Schultz, J., Kwiterovich, P., Shan, B., Barnes, R., and Hobbs, H. H. (2000) Accumulation of dietary cholesterol in sitosterolemia caused by mutations in adjacent ABC transporters. *Science 290*, 1771–1775.
4. Lee, M. H., Lu, K., Hazard, S., Yu, H., Shulenin, S., Hidaka, H., Kojima, H., Allikmets, R., Sakuma, N., Pegoraro, R., Srivastava, A. K., Salen, G., Dean, M., and Patel, S. B. (2001) Identification of a gene, ABCG5, important in the regulation of dietary cholesterol absorption. *Nat. Genet. 27*, 79–83.
5. Yu, L., Hammer, R. E., Li-Hawkins, J., von Bergmann, K., Lutjohann, D., Cohen, J. C., and Hobbs, H. H. (2002) Disruption of Abcg5 and Abcg8 in mice reveals their crucial role in biliary cholesterol secretion. *Proc. Natl. Acad. Sci. U.S.A. 99*, 16237–16242.
6. Yu, L., Li-Hawkins, J., Hammer, R. E., Berge, K. E., Horton, J. D., Cohen, J. C., and Hobbs, H. H. (2002) Overexpression of ABCG5 and ABCG8 promotes biliary cholesterol secretion and reduces fractional absorption of dietary cholesterol. *J. Clin. Invest. 110*, 671–680.
7. Kosters, A., Frijters, R. J., Schaap, F. G., Vink, E., Plosch, T., Ottenhoff, R., Jirsa, M., de Cuyper, I. M., Kuipers, F., and Groen, A. K. (2003) Relation between hepatic expression of ATP-binding cassette transporters G5 and G8 and biliary cholesterol secretion in mice. *J. Hepatol. 38*, 710–716.
8. Plosch, T., Bloks, V. W., Terasawa, Y., Berdy, S., Siegler, K., van der Sluijs, F., Kema, I. P., Groen, A. K., Shan, B., Kuipers, F., and Schwarz, M. (2004) Sitosterolemia in ABC-transporter G5-deficient mice is aggravated on activation of the liver-X receptor. *Gastroenterology 126*, 290–300.
9. Klett, E. L., Lu, K., Kosters, A., Vink, E., Lee, M. H., Altenburg, M., Shefer, S., Batta, A. K., Yu, H., Chen, J., Klein, R., Looije, N., Oude-Elferink, R., Groen, A. K., Maeda, N., Salen, G., and Patel, S. B. (2004) A mouse model of sitosterolemia: absence of Abcg8/sterolin-2 results in failure to secrete biliary cholesterol. *BMC Med. 2*, 5.
10. Wu, J. E., Basso, F., Shamburek, R. D., Amar, M. J., Vaisman, B., Szakacs, G., Joyce, C., Tansey, T., Freeman, L., Paigen, B. J.,

Thomas, F., Brewer, H. B., Jr., and Santamarina-Fojo, S. (2004) Hepatic ABCG5 and ABCG8 overexpression increases hepatobiliary sterol transport but does not alter aortic atherosclerosis in transgenic mice. *J. Biol. Chem. 279*, 22913–22925.

11. Wang, J., Sun, F., Zhang, D.-w., Ma, Y., Xu, F., Belani, J. D., Cohen, J. C., Hobbs, H. H., and Xie, X.-S. (2006) Sterol transfer by ABCG5 and ABCG8: In vitro assay and reconstitution. *J. Biol. Chem. 281*, 27894–27904.

12. Zhang, D. W., Graf, G. A., Gerard, R. D., Cohen, J. C., and Hobbs, H. H. (2006) Functional asymmetry of nucleotide-binding domains in ABCG5 and ABCG8. *J. Biol. Chem. 281*, 4507–4516.

13. Yu, L., von Bergmann, K., Lutjohann, D., Hobbs, H. H., and Cohen, J. C. (2004) Selective sterol accumulation in ABCG5/ABCG8-deficient mice. *J. Lipid Res. 45*, 301–307.

14. Kipp, H., and Arias, I. M. (2000) Newly synthesized canalicular ABC transporters are directly targeted from the Golgi to the hepatocyte apical domain in rat liver. *J. Biol. Chem. 275*, 15917–15925.

15. Inoue, M., Kinne, R., Tran, T., Biempica, L., and Arias, I. M. (1983) Rat liver canalicular membrane vesicles. Isolation and topological characterization. *J. Biol. Chem. 258*, 5183–5188.

16. Xie, X. S., and Stone, D. K. (1986) Isolation and reconstitution of the clathrin-coated vesicle proton translocating complex. *J. Biol. Chem. 261*, 2492–2495.

17. Aronson, N. N., and Touster, O. (1974) Isolation of rat liver plasma membrane fragments in isotonic sucrose. *Methods Enzymol. 31*, 90–102.

18. Kawate, N., and Menon, K. M. (1994) Palmitoylation of luteinizing hormone/human choriogonadotropin receptors in transfected cells. Abolition of palmitoylation by mutation of Cys-621 and Cys-622 residues in the cytoplasmic tail increases ligand-induced internalization of the receptor. *J. Biol. Chem. 269*, 30651–30658.

19. Ihrke, G., Neufeld, E. B., Meads, T., Shanks, M. R., Cassio, D., Laurent, M., Schroer, T. A., Pagano, R. E., and Hubbard, A. L. (1993) WIF-B cells: An *in vitro* model for studies of hepatocyte polarity. *J. Cell Biol. 123*, 1761–1775.

20. Sai, Y., Nies, A. T., and Arias, I. M. (1999) Bile acid secretion and direct targeting of mdr1-green fluorescent protein from Golgi to the canalicular membrane in polarized WIF-B cells. *J. Cell Sci. 112*, 4535–4545.

21. Wang, Z., Stalcup, L. D., Harvey, B. J., Weber, J., Chloupkova, M., Dumont, M. E., Dean, M., and Urbatsch, I. L. (2006) Purification and ATP hydrolysis of the putative cholesterol transporters ABCG5 and ABCG8. *Biochemistry 45*, 9929–9939.

22. Graf, G. A., Cohen, J. C., and Hobbs, H. H. (2004) Missense mutations in ABCG5 and ABCG8 disrupt heterodimerization and trafficking. *J. Biol. Chem. 279*, 24881–24888.

23. Ozvegy, C., Varadi, A., and Sarkadi, B. (2002) Characterization of drug transport, ATP hydrolysis, and nucleotide trapping by the human ABCG2 multidrug transporter. Modulation of substrate specificity by a point mutation. *J. Biol. Chem. 277*, 47980–47990.

24. Takahashi, K., Kimura, Y., Kioka, N., Matsuo, M., and Ueda, K. (2006) Purification and ATPase activity of human ABCA1. *J. Biol. Chem. 281*, 10760–10768.

25. Schmidt, M., Schmidt, M. F., and Rott, R. (1988) Chemical identification of cysteine as palmitoylation site in a transmembrane protein (Semliki Forest virus E1). *J. Biol. Chem. 263*, 18635–18639.

26. Davidson, A. L., and Maloney, P. C. (2007) ABC transporters: How small machines do a big job. *Trends Microbiol. 15*, 448–455.

27. Sun, H., Molday, R. S., and Nathans, J. (1999) Retinal stimulates ATP hydrolysis by purified and reconstituted ABCR, the photoreceptor-specific ATP-binding cassette transporter responsible for Stargardt disease. *J. Biol. Chem. 274*, 8269–8281.

28. Mao, Q., Deeley, R. G., and Cole, S. P. (2000) Functional reconstitution of substrate transport by purified multidrug resistance protein MRP1 (ABCC1) in phospholipid vesicles. *J. Biol. Chem. 275*, 34166–34172.

29. Hollenstein, K., Dawson, R. J., and Locher, K. P. (2007) Structure and mechanism of ABC transporter proteins. *Curr. Opin. Struct. Biol. 17*, 412–418.

30. Xu, J., Liu, Y., Yang, Y., Bates, S., and Zhang, J.-T. (2004) Characterization of oligomeric human half-ABC transporter ATP-binding cassette G2. *J. Biol. Chem. 279*, 19781–19789.

31. Trompier, D., Alibert, M., Davanture, S., Hamon, Y., Pierres, M., and Chimini, G. (2006) Transition from dimers to higher oligomeric forms occurs during the ATPase cycle of the ABCA1 transporter. *J. Biol. Chem. 281*, 20283–20290.

32. Linder, M. E., and Deschenes, R. J. (2007) Palmitoylation: Policing protein stability and traffic. *Nat. Rev. Mol. Cell. Biol. 8*, 74–84.

33. Fukata, M., Fukata, Y., Adesnik, H., Nicoll, R. A., and Bredt, D. S. (2004) Identification of PSD-95 palmitoylating enzymes. *Neuron 44*, 987–996.

34. Fernandez-Hernando, C., Fukata, M., Bernatchez, P. N., Fukata, Y., Lin, M. I., Bredt, D. S., and Sessa, W. C. (2006) Identification of Golgi-localized acyl transferases that palmitoylate and regulate endothelial nitric oxide synthase. *J. Cell Biol. 174*, 369–377.

35. Smotrys, J. E., and Linder, M. E. (2004) Palmitoylation of intracellular signaling proteins: Regulation and function. *Annu. Rev. Biochem. 73*, 559–587.

36. Takada, T., Suzuki, H., and Sugiyama, Y. (2005) Characterization of polarized expression of point- or deletion-mutated human BCRP/ABCG2 in LLC-PK1 cells. *Pharm. Res. 22*, 458–464.

37. Small, D. M. (2003) Role of ABC transporters in secretion of cholesterol from liver into bile. *Proc. Natl. Acad. Sci. U.S.A. 100*, 4–6.

38. Vrins, C., Vink, E., Vandenberghe, K. E., Frijters, R., Seppen, J., and Groen, A. K. (2007) The sterol transporting heterodimer ABCG5/ABCG8 requires bile salts to mediate cholesterol efflux. *FEBS Lett. 581*, 4616–4620.

39. van Driel, I. R., Davis, C. G., Goldstein, J. L., and Brown, M. S. (1987) Self-association of the low density lipoprotein receptor mediated by the cytoplasmic domain. *J. Biol. Chem. 262*, 16127–16134.